

**Cementitious Grouts for ILW Encapsulation - Hydration & Continuity of Supply within the UK – 16184**

Josh Hawthorne \*, Gavin Cann \*\*, Leon Black \*

\* University of Leeds

\*\* National Nuclear Lab

**ABSTRACT**

In the UK the preferred route to disposal for the majority of intermediate level nuclear waste (ILW) streams is encapsulation within a cementitious matrix, accounting for 83% of waste conditioned to date (NDA, 2013). The method is well-defined and produces a waste package that is both chemically and physically stable, providing a multi-layered barrier to the release of the waste species contained within. Due to the process of treatment, facilitated via remote operation, it is necessary for the grouting matrices to meet strict performance limits in terms of their flow, setting time and avoidance of the formation of bleed water or segregation. To this end, the limits on composition of the anhydrous materials (a mixture of ordinary Portland cement [OPC] and blastfurnace slag [BFS]) are tight to ensure conformity.

Whilst these limits on composition are well understood, their impact upon grout hydration, and hence performance, is poorly defined. This study investigates the effects of modifying the physical and chemical composition of both the OPC and the BFS components of the matrix in order to identify the sensitivity or otherwise of the system to ensure that a continuity of supply is maintained.

A number of techniques, scanning electron microscopy - image analysis (SEM-IA), chemical shrinkage (measured via dilatometry), isothermal conduction calorimetry (ICC), thermogravimetric analysis (TGA) and X-ray diffraction (XRD), have been applied to assess the rate and degree of hydration (DoH) of a range of grouts prepared with OPC and BFS with a range of chemical and physical compositions. This has been coupled with subsequent engineering performance testing, with additional analysis to understand the impact of a fire scenario within a storage or disposal facility, to provide an indication towards the resilience of the waste packages to a potential catastrophic event.

**INTRODUCTION**

Encapsulation within a cementitious grout is the preferred conditioning method for ILW within the UK (Wilson, 1996, Glasser, 2011, Glasser, 1992) owing to the rheological properties of the encapsulant prior to setting and the chemical and physical barrier to release of contaminants that the hardened product provides (Shi and Fernandez-Jimenez, 2006, Collier et al., 2006). The anhydrous materials which are used to form the grouting matrices must conform to strict physical and chemical compositional limits. As a result of these tight parameters on composition, and highlighted by previous experience, continuity of supply is a potential risk.

Investigating potential replacement suppliers and sources of both OPC and BFS has been, and continues to be, a significant area of research industrially and is one of the key drivers behind the current study.

Quantifying the effects of compositional changes is essential to determine the resilience to current and future changes in supply. Furthermore, a clear and thorough understanding of the rate and degree of hydration of these materials is not well established. It has been shown that at high levels of replacement, hydration of BFS is diminished significantly (Gruyaert, 2011) but until recently there have been difficulties in accurately determining degree of hydration of supplementary cementitious material (SCMs) [in this instance BFS, but also including pulverised fly ash (PFA), silica fume (SF), metakaolin (MK) etc.] in blended systems (Scrivener et al., 2015). Recently, a range of techniques have been used to accurately follow the hydration of the various phases within these complex, dynamic systems (Whittaker, 2014, Kocaba, 2010). This will help to provide the strong, clear understanding necessary if we are to ensure that wastes are adequately treated and pose little to no residual risk to either the population or the environment.

One of the key concerns for the long-term suitability and performance of waste packages is their resilience to potential catastrophic events within a storage or disposal facility. A number of conformity tests have been developed (IAEA, 2012), including fire performance. To compare materials and to gain an insight into how composition might affect resilience to deleterious environments, a range of samples have been subjected to conditions in line with those outlined by the IAEA, with subsequent engineering performance testing to assess the impact of elevated temperature on permeability through changes induced upon the microstructure by phase dehydration. All of this provides the foundations for understanding the intimate and complex relationships between composition, hydration, microstructure and performance.

## **MATERIALS AND METHODS**

Two OPC and 3 BFS powders were used throughout the project; offering a comparison in terms of both physical (fineness and specific surface area) and chemical composition. Mixes were prepared in line with the most common grout specification used industrially within the UK for treatment of ILW, with 75% replacement by BFS and at a water/binder ratio (w/b) of 0.35.

Six mixes were prepared ( $C_1S_1$ ,  $C_2S_1$ ,  $C_1S_{2c}$ ,  $C_2S_{2c}$ ,  $C_1S_{2f}$  and  $C_1S_{3c}$ ) where numeric subscript indicate the different sources of cement (C) and blast furnace slag (S) and 'c' and 'f' denote whether the slag is at the coarse or fine material limit. The current and legacy specifications ( $C_2S_1$  and  $C_1S_1$  respectively) are slightly more complex in that the slag fraction ( $S_1$ ), which accounts for 75% of the powder volume, is a mix of granular slag 'Calumite',  $d_{0.5} = 330\mu\text{m}$  which accounts for 35% by weight of the BFS fraction, and 65% Scunthorpe BFS which is much finer and lies outside of the specification. This ensures that suitable rheological properties are maintained without a modification to w/b.

The physical characteristics of the anhydrous materials are illustrated in TABLE I and FIGURE I, chemical composition, determined via fused-bead XRF is provided in

TABLE 2.

TABLE I: Physical composition of anhydrous materials

| Material              | SSA (m <sup>2</sup> /Kg) | d <sub>0.5</sub> (µm) | Density (g/cm <sup>3</sup> ) |
|-----------------------|--------------------------|-----------------------|------------------------------|
| C1                    | 325                      | 17.77                 | 3.16                         |
| C2                    | 384                      | 15.73                 | 3.15                         |
| S1 fine (65%)         | 526                      | 7.33                  | 2.95                         |
| S1 extra coarse (35%) |                          | 330                   | 2.80                         |
| S2c                   | 242                      | 41.07                 | 2.91                         |
| S3c                   | 294                      | 39.17                 | 2.83                         |
| S2f                   | 419                      | 16.32                 | 2.93                         |

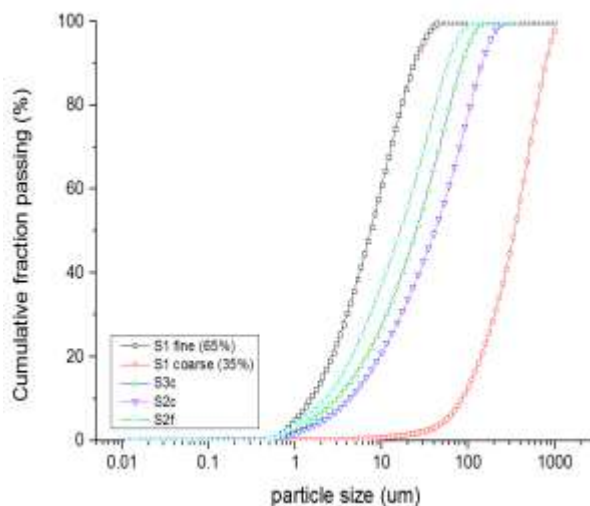


FIGURE I: Particle size distribution for anhydrous materials

TABLE 2: Chemical composition of anhydrous materials and basicity ratios of BFS powders

| Phase (%)                      | C1    | C2    | S1f   | S1c/S3c | S2c/S2f |
|--------------------------------|-------|-------|-------|---------|---------|
| CaO                            | 65.37 | 64.63 | 39.76 | 40.52   | 43.24   |
| SiO <sub>2</sub>               | 21.05 | 20.27 | 37.15 | 36.03   | 36.13   |
| Al <sub>2</sub> O <sub>3</sub> | 4.46  | 5.19  | 10.81 | 11.77   | 10.76   |
| TiO <sub>2</sub>               | 0.38  | 0.25  | 0.74  | 0.89    | 0.72    |
| MnO                            | 0.07  | 0.04  | 0.41  | 0.41    | 0.36    |
| Fe <sub>2</sub> O <sub>3</sub> | 2.75  | 2.61  | 0.41  | 0.25    | 0.52    |
| MgO                            | 0.98  | 2.36  | 7.86  | 7.92    | 3.74    |
| K <sub>2</sub> O               | 0.67  | 0.79  | 0.64  | 0.56    | 0.94    |
| Na <sub>2</sub> O              | 0.33  | 0.39  | 0.21  | 0.25    | 0.16    |
| SO <sub>3</sub>                | 3.40  | 2.84  | 1.66  | 0.64    | 0.61    |
| Basicity ratios                |       |       |       |         |         |
| C/S                            |       |       | 1.070 | 1.125   | 1.197   |
| (C+Mg)/S                       |       |       | 1.282 | 1.344   | 1.300   |
| (C+Mg+Al)/S                    |       |       | 1.573 | 1.671   | 1.598   |

Heat evolution was followed for all mixes over 28 days using a TamAir 8 isothermal calorimeter. In order to isolate the heat attributable to the different phases, each system was also run with the BFS component replaced by inert quartz. This allows for the 'filler effect' (Costoya, 2008) to be accounted for, since the quartz provides nucleation sites on which the OPC within the system can hydrate and ensures that the water: OPC ratio remains equal.

### Following hydration via dilatometry

Chemical shrinkage (see FIGURE II) was measured in triplicate via dilatometry, as described by (Geiker, 1983) and further developed and optimised by (Whittaker, 2014). The method works on the principle that water has a lower specific volume when bound to a solid than when a free liquid.

Samples were prepared and placed in plastic vials (15g of grout per sample), with deionised water carefully placed on top. A rubber bung, fitted with a 1ml pipette, was used to seal the system and a drop of oil placed on top of the water within the pipette. The oil serves two purposes, first it ensures that no water leaks from the system due to evaporation and secondly it is used as a tracer for subsequent image analysis from the images taken remotely via webcam throughout the experiment.

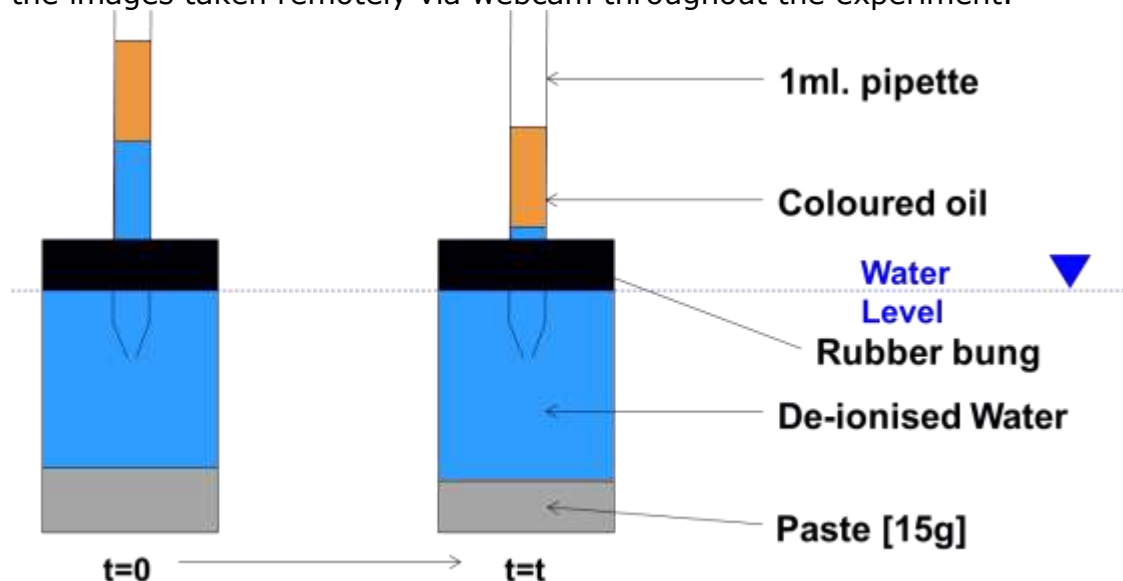


**FIGURE II: Schematic of experimental setup for measuring chemical shrinkage**

### Degree of hydration (via SEM)

SEM images were acquired in backscattered mode (BSE) from samples hydrated for 2, 7, 14 & 28 days. 50 images were taken per sample, at 800x magnification, a working distance of 8mm and 15keV accelerating voltage. Previous studies have

performed segmentation on the micrographs in order to quantify the volume of residual unreacted material (Utton, 2006, Brough and Atkinson, 2000).

Given the complexity of the materials analysed within the study it was necessary to introduce a further step in order to properly isolate the anhydrous BFS. Mg maps at a nominal count rate of 30k cps for 2-3 minutes per image were collected and were overlaid onto the thresholded micrograph to allow for further segmentation, as illustrated in Figure III. All analysis, segmentation and thresholding was carried out using ImageJ.

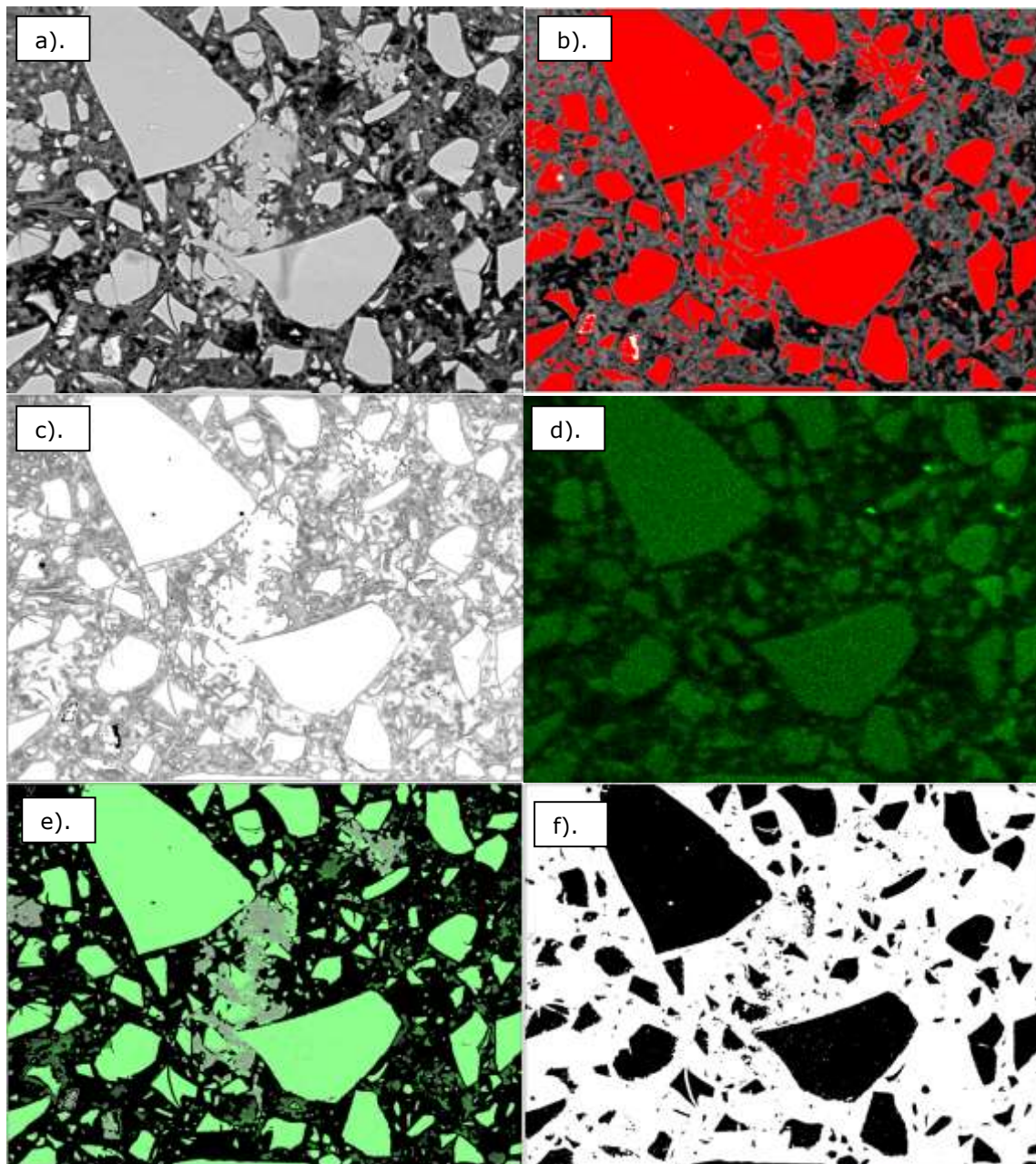


**Figure III: SEM images. a). Original micrograph. b). First segmentation, including anhydrous BFS, anhydrous OPC and calcium hydroxide (CH). c). Inversion of b. d). Corresponding Mg map. e). Micrograph with Mg. map overlain at 20% opacity. f). Final image, showing only residual anhydrous BFS.**

## **Fire resistance testing**

All mixes were heat tested in triplicate at a range of temperatures to simulate a fire scenario. Testing was developed from IAEA conformity tests and informed by the testing protocols of the Radioactive Waste Management Limited (RWM) requirements for a geological disposal facility (GDF) in the UK (NDA, 2010). It was neither possible nor feasible to conduct testing on full-scale waste packages, instead much smaller samples were analysed and as such the results provide may be seen to reflect a severe 'worst case' scenario and give an indication towards the impact of such a scenario on the outer surface of large waste packages.

Samples (25mm Ø and 40mm in height) were heated to 200°, 400° and 800°C and held for a dwell time of 30 minutes before being cooled in air. Samples were weighed and measured to determine any dimensional and mass changes induced by the treatment and were subsequently placed into an oven in air at 50°C until constant mass, at which point it was assumed all unbound water had been driven off.

Following heat treatment, the intrinsic permeability of the samples was calculated using a gas permeameter developed at the University of Leeds, the Leeds cell (Cabrera and Lynsdale, 1988). The samples are loaded into a sealed system and gas (N<sub>2</sub> in this case) is forced through at a known pressure. When the flow has stabilised through the sample, the time taken for a known volume of gas is calculated with the aid of a bubble flow meter. The rate of gas flow is calculated at 3 applied pressures and for 3 samples per mix; from this, the intrinsic permeability is calculated. To provide a means of simple comparison, an intrinsic permeability coefficient may be calculated (a  $-\log_{10}$  value). A visual inspection was also conducted and images taken to provide a comparison across mix designs.

Samples were also prepared for X-ray micro-computational tomography (X-ray  $\mu$ CT) in quartz glass capillaries (5mm Ø) and imaged at 7 and 28 days. A number of samples, aged to 28 days, were heat treated to 400° and 800°C in line with samples for permeability testing. Analysis was performed at NNL central lab using a Bruker Skyscan 1172 machine; source voltage was maintained at 80 kV and a current of 125  $\mu$ A. 450 projections at a step size of 0.4° and an exposure time of 5.5 s each were acquired on an 11Mp CCD camera. The pixel resolution under these conditions was between 1.2 and 1.4  $\mu$ m. Some preliminary data from this testing are included, however quantifiable results are not yet available.

## **RESULTS**

Within each of the 6 mix designs investigated, the reaction of the OPC component was accelerated at early age as a result of the filler effect and, with the less reactive BFS accounting for 75% of the powder fraction of the mixes, the high water to cement ratio (w/c). This rapid hydration of the OPC led to conditions favourable for the hydration of the BFS component of each system, namely the increase in pH and production of Portlandite (CH) which is subsequently consumed by the BFS to form

secondary C-S-H within the composite matrix.

Slag fineness had a clear impact on hydration behaviour. The finer BFS (S2f) accelerated the hydration of the OPC through its higher surface area providing more nucleation sites. The result can be observed in FIGURE IV where the onset of hydration occurs sooner and to a greater degree. The continued heat evolution within this mix remains higher than for the mix C1S2c over the first few days, due in part to an elevated rate of BFS hydration. After 7-10 days the rate of heat release is comparable across the two mixes, in agreement with the results obtained for SEM-IA.

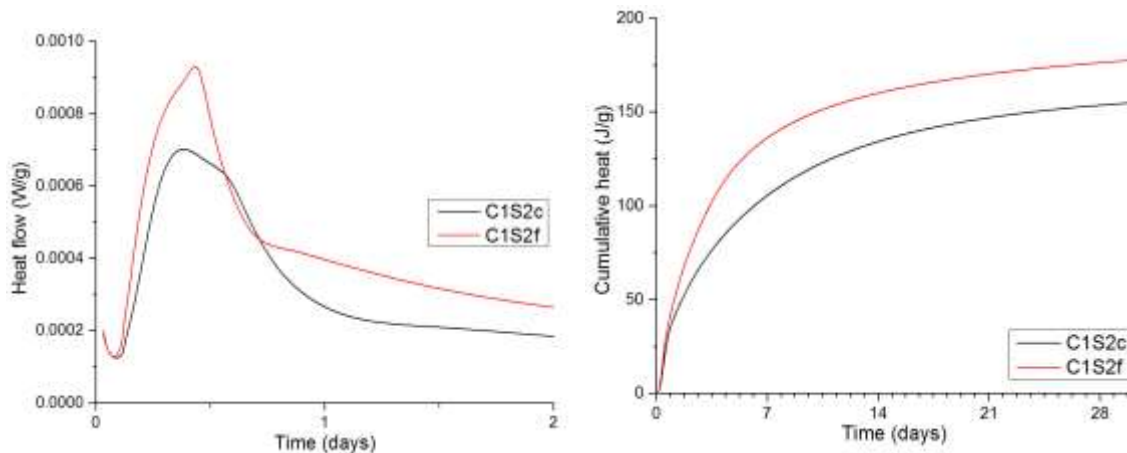


**FIGURE IV: ICC data for mixes C1S2c & C1S2f**

The application of indirect techniques, such as ICC or chemical shrinkage via dilatometry provides very accurate results and allow for materials to be analysed in real time over extended periods. However, to provide reliability in results they should be calibrated against direct techniques (such as SEM-IA).

Quantifying degree of hydration via SEM-IA (when coupled with EDX mapping data) has been shown to be a very powerful technique and provides very good, reliable results when analysing more mature samples (28 days+). The key drawbacks of this method are the time taken to perform the analysis and the requirement of expensive, sophisticated machines to provide high quality images and high resolution map data from EDX. Furthermore, the technique has been shown to overestimate degree of BFS hydration at early age (Kocaba, 2010, Whittaker, 2014) due to limitations in resolution and therefore loss of accuracy in identifying small volumes of anhydrous materials.

FIGURE V shows the results from all three techniques when applied to samples C1S2c and C1S2f; with all methods showing that the fineness and degree of comminution of the BFS has a significant impact upon its early age hydration. The results here for both ICC and chemical shrinkage show the heat released or chemical shrinkage as a result of only the hydration of the BFS.

As in previous studies, the results from SEM-IA provide a slight over-estimation of

degree of hydration at early age, however there appears to be good agreement across all three techniques. The very low values of heat or shrinkage detected highlight the sensitivity of these indirect methods to changes within the systems.

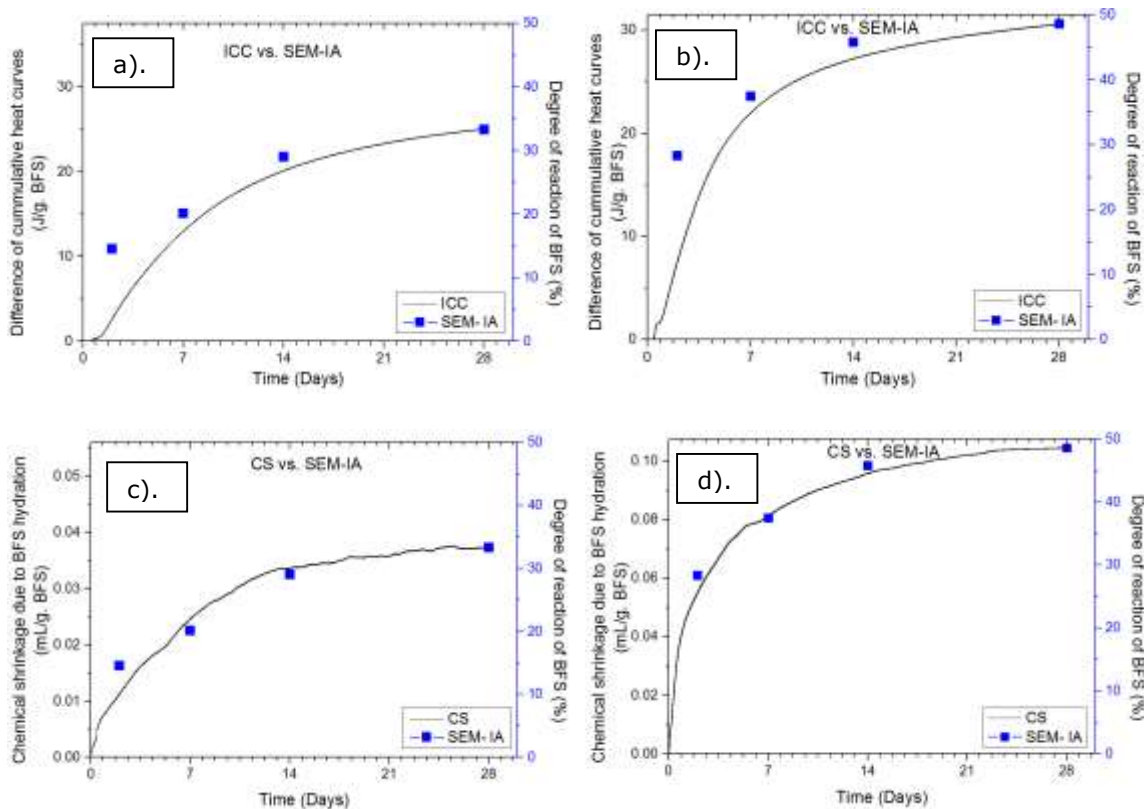


**FIGURE V: a). ICC vs. SEM for C1S2c. b). ICC vs. SEM for C1S2f. c). CS vs. SEM for C1S2c. d). CS vs. SEM for S1S2f.**

The results illustrated in FIGURE VI further highlights the accuracy of each technique and illustrates the improvements that have been made to the technique and sample preparation protocol for measuring chemical shrinkage over recent years (Geiker, 1983, Kocaba, 2010, Whittaker, 2014).

The hydration of BFS within the composite grouts at high levels of replacement is governed by a number of factors. The most significant parameter appears to be the fineness of grinding, which affects both the rate and degree of hydration of the BFS component at early to medium age. The type of cement, including both its chemical and physical composition has some bearing on early age BFS hydration. In this study a finer OPC generally results in a higher degree of BFS hydration at early age, however following continued hydration the disparity decreases as the chemistry becomes the dominant factor.



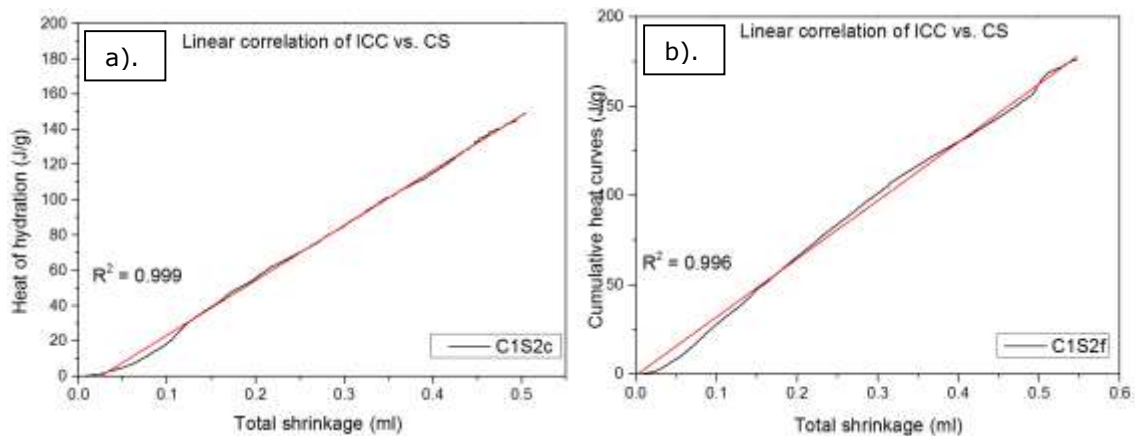


FIGURE VI: a). ICC vs. CS for C1S2c. b). ICC vs. CS for C1S2f.

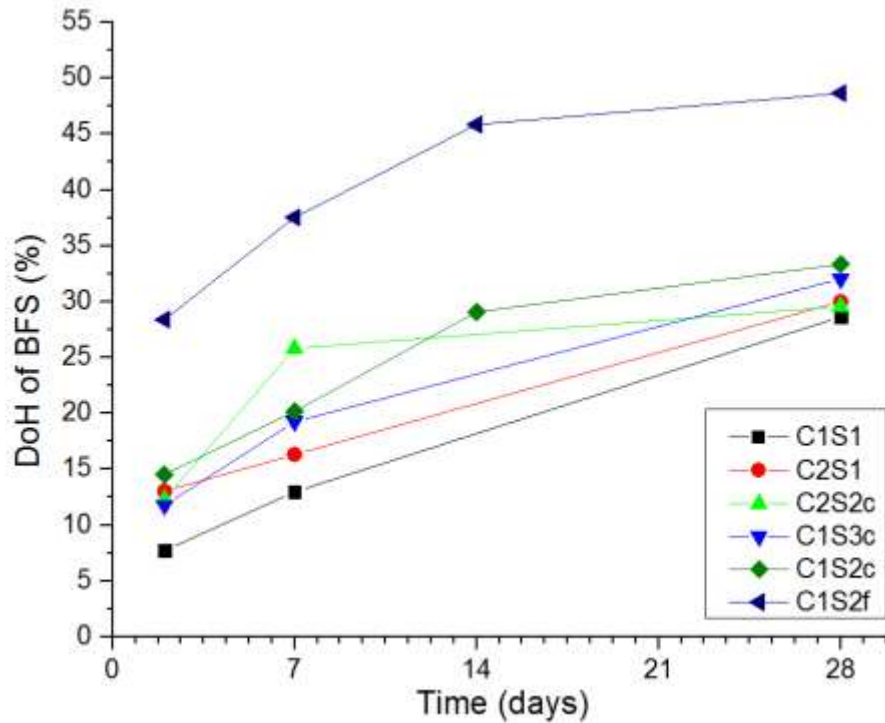
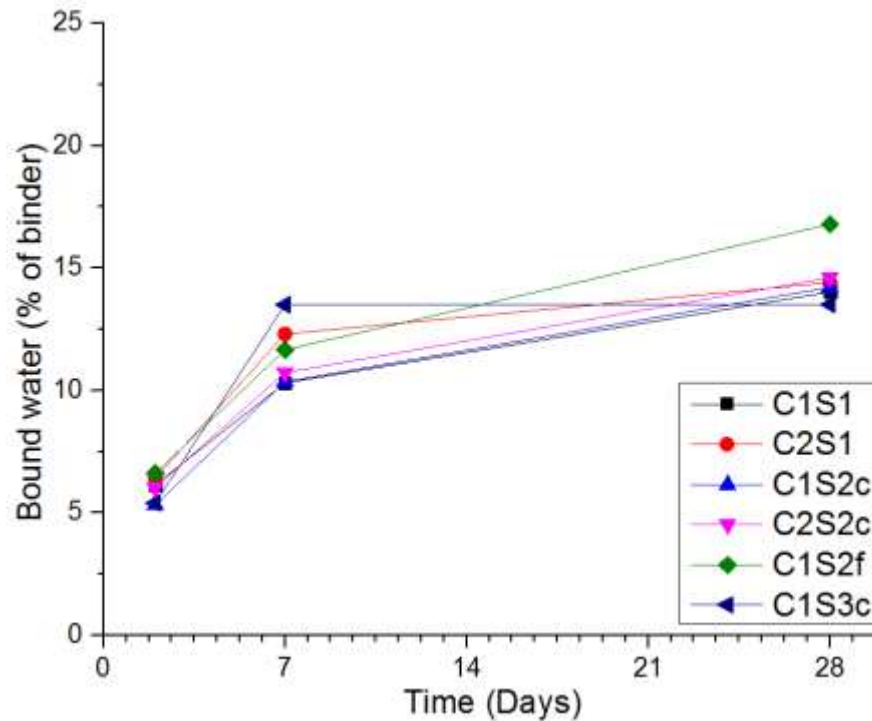


FIGURE VII: Quantitative degree of hydration of BFS within each system from SEM-IA

The figures calculated for DoH here are in line with those determined in previous studies, where replacement levels are 75% and 28 day DoH values are in the range of 28 – 49%. At 40% replacement, (Kocaba, 2010) observed values between 35 and 55% DoH at 28 days; (Lumley et al., 1996) measured DoH to be in the range 30-55% at a range of BFS contents up to 69% and found that (as would be expected) increasing BFS content generally leads to a lower overall DoH. (Whittaker, 2014) determined DoH data in the range 42-53% at replacement levels from 40-70% by BFS at 28 days.

A further method which provides insight into hydration is the calculation of bound water (FIGURE VIII); however, it does not allow for direct quantification of overall hydration of that of distinct phases with composite systems (Pane and Hansen, 2005).



**FIGURE VIII: Bound water content of all mixes at early age**

FIGURE IX illustrates the intrinsic permeability coefficients for all mixes following a range of heat treatment protocols. The samples heated to 800°C were too severely damaged and cracked to allow for testing via this method, images of some of the cracked samples are given in FIGURE X. What may be garnered from FIGURE IX is that heating to 200°C appears to reduce permeability; whilst this result was not expected it is believed to be the result of a densification within the samples, and a coarsening of the interconnectivity within the pore structure; this is to be quantified via X-ray CT analysis.

It is expected that the exposure time of 30 minutes is likely to not have had too detrimental an effect upon the samples at 200°C, and it is not until they are exposed to 400°C that significant damage is caused.

As is visible in FIGURE X, the disparity in cracking across the samples appears high. Samples prepared with the NNL specification materials appear to be more adversely affected by heating to 800°C. Our predictions are that this is a result of the large 'Calumite' grains within these systems (this appears to be the case judging by preliminary X-ray CT analysis). It seems that the cracks are

propagating around these large grains, suggesting that there exists something of an interfacial transition zone and a less dense hydration product around the grains.

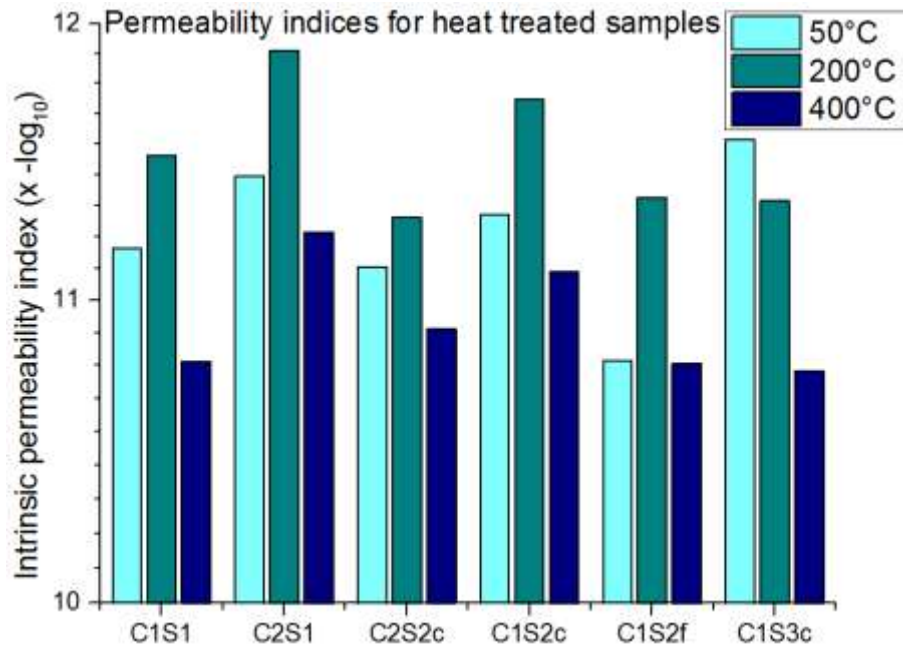
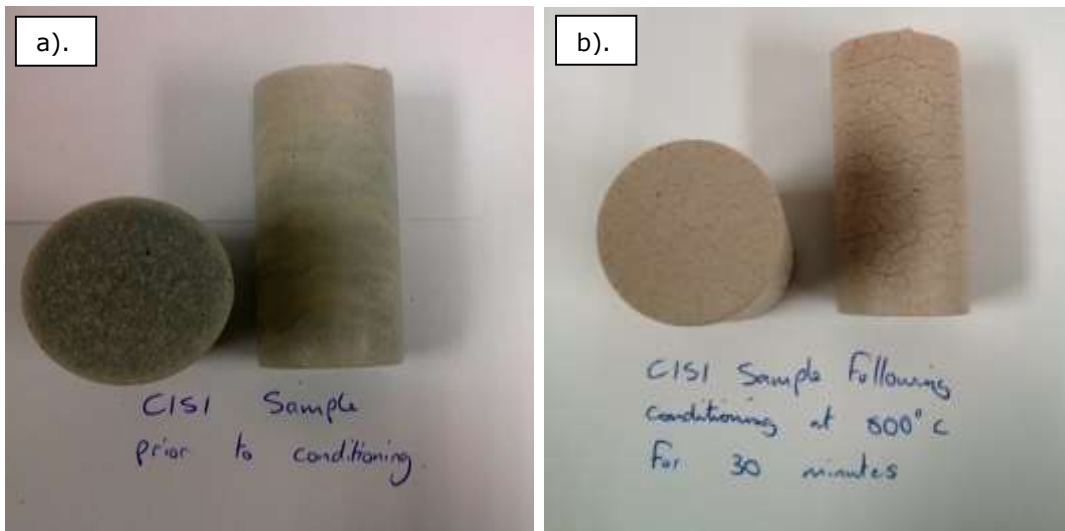


FIGURE IX: Intrinsic permeability of heat treated samples determined via Leeds cell.





**FIGURE X: a). C1S1 at 28 days. b). C1S1 following heating to 800°C. c). C1S2c at 28 days d). C1S2c following heating to 800°C.**

FIGURE XI shows 3-D reconstructions of samples at 28 days. This visual aid shows the large disparity in particle size between the Calumite grains and the more regular particle size distribution within the C1S2c system. Work is ongoing to complete quantification; including segmentation, thresholding and random walk simulations to assess the interconnectivity of the pore network and how these parameters are affected with time and as a result of heat treatment (to simulate a fire within a storage facility).

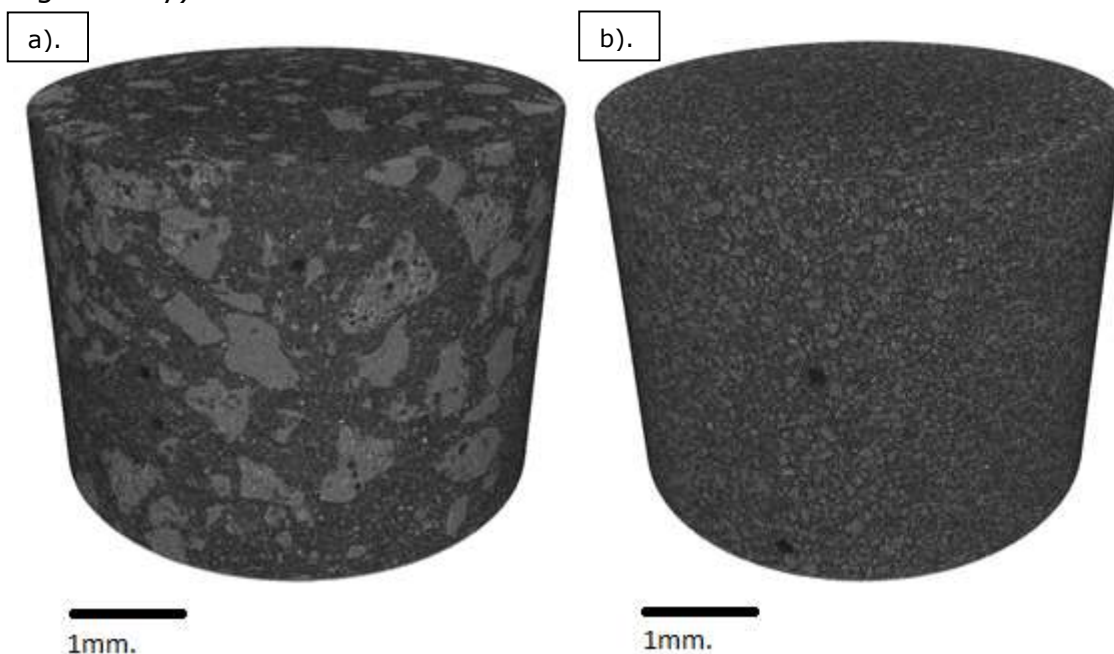


**FIGURE XI: a). C2S1 at 28 days. b). C1S2c at 28 days**

## **CONCLUSIONS**

The results obtained in this study highlight that the methods used to quantify the hydration of more traditional construction cements and composites are suitable for assessing and comparing the hydration of the grouts used for the treatment of ILW in the UK.

By analyzing mixes prepared with BFS powders of either differing chemical or physical composition independent of one another (ie. S2c vs. S2f and S2c vs S3c) we are able to determine that BFS fineness plays a much greater role in determining hydration, at early age, than chemical composition. The chemical composition of anhydrous materials remains highly significant since this determines the thermodynamics of hydration and governs the hydration products formed within the system, ultimately impacting upon the resilience of a waste package.

Whilst a fire or other catastrophic event within a storage or disposal scenario seems unlikely, a thorough understanding of its implications remains imperative. It would appear from this study that the current specification grouting matrix, with its fraction of larger BFS grains, is more susceptible to cracking and/or spalling at elevated temperatures due to the propagation of cracks around these larger particles

The overall degree of hydration of the constituent phases present, whilst slightly lower than for the other mixes studied here, remain comparable. Further research is ongoing to elucidate any impact that these changes in composition have upon the microstructure, in particular the porosity. This insight is key in beginning to understand the transport properties of waste packages and how susceptible, or otherwise, they are to changes in composition as well as their resilience to deleterious environments.

**REFERENCES**

- BROUGH, A. R. & ATKINSON, A. 2000. Automated identification of the aggregate-paste interfacial transition zone in mortars of silica sand with Portland or alkali-activated slag cement paste. *Cement and Concrete Research*, 30, 849-854.
- CABRERA, J. G. & LYNSDALE, C. J. 1988. A new gas permeameter for measuring the permeability of mortar and concrete. *Magazine of Concrete Research*, 40, 177-182.
- COLLIER, N. C., MILESTONE, N. B., HILL, J. & GODFREY, I. H. 2006. The disposal of radioactive ferric floc. *Waste Management*, 26, 769-775.
- COSTOYA, M. 2008. *Effect of particle size distribution on the hydration kinetics and microstructural development of cement hydration*. Ph.D. Thesis, Ecole Polytechnique Federale De Lausanne
- GEIKER, M. 1983. *Studies of Portland cement hydration by measurements of chemical shrinkage and a systematic evaluation of hydration curves by means of the dispersion method*. Ph.D. Thesis, Technical University of Denmark.
- GLASSER, F. P. 1992. Progress in the immobilization of radioactive wastes in cement. *Cement and Concrete Research*, 22, 201-216.
- GLASSER, F. P. 2011. *Application of inorganic cements to the conditioning and immobilisation of radioactive wastes*.
- GRUYAERT, E. 2011. *Effect of blast-furnace slag as cement replacement on hydration, microstructure, strength and durability of concrete*. Ph.D. Thesis, Ghent University.
- IAEA 2012. Regulations for the Safe Transport of Radioactive Material: 2012 Edition. Vienna, Austria.
- KOCABA, V. 2010. *Development and Evaluation of Methods to Follow Microstructural Development of Cementitious Systems Including Slags*. Ph.D. Thesis, Ecole Polytechnique Federale De Lausanne.
- LUMLEY, J. S., GOLLOP, R. S., MOIR, G. K. & TAYLOR, H. F. W. 1996. Degrees of reaction of the slag in some blends with Portland cements. *Cement and Concrete Research*, 26, 139-151.
- NDA 2010. Geological Disposal: Waste package accident performance status report.
- NDA 2013. 2013 UK Radioactive Waste Inventory - A Summary of the 2013 Inventory.
- PANE, I. & HANSEN, W. 2005. Investigation of blended cement hydration by isothermal calorimetry and thermal analysis. *Cement and Concrete Research*, 35, 1155-1164.

SCRIVENER, K. L., LOTHENBACH, B., DE BELIE, N., GRUYAERT, E., SKIBSTED, J., SNELLINGS, R. & VOLLPRACHT, A. 2015. TC 238-SCM: hydration and microstructure of concrete with SCMs. *Materials and Structures*, 48, 835-862.

SHI, C. & FERNANDEZ-JIMENEZ, A. 2006. Stabilization/solidification of hazardous and radioactive wastes with alkali-activated cements. *Journal of Hazardous Materials*, 137, 1656-63.

UTTON, C. A. 2006. *The encapsulation of a BaCO<sub>3</sub> waste in composite cement*. PhD Thesis, University of Sheffield.

WHITTAKER, M. 2014. *The Impact of Slag Composition on the microstructure of Composite Slag Cements Exposed to Sulfate Attack*. Ph.D. Thesis, University of Leeds.

WILSON, P. D. 1996. *The Nuclear Fuel Cycle: From Ore to Wastes* Oxford, Oxford University Press.